Journal of Electromagnetic Analysis and Applications, 2021, 13, 67-81
https://www.scirp.org/journal/jemaa
ISSN Online: 1942-0749
ISSN Print: 1942-0730

AC Back Surface Recombination Velocity in n^+-p-p^+ Silicon Solar Cell under Monochromatic Light and Temperature

Mame Faty Mbaye Fall[1], Idrissa Gaye[2], Dianguina Diarisso[2], Gora Diop[3], Khady Loum[1], Nafy Diop[1], Khalidou Mamadou Sy[3], Mor Ndiaye[3], Gregoire Sissoko[3]

[1]Ecole Polytechnique de Thiès, Thiès, Sénégal
[2]Institute of Technology, University of Thiès, Thiès, Sénégal
[3]Laboratory of Semiconductors and Solar Energy, Physics Department, Faculty of Science and Technology, University Cheikh Anta Diop, Dakar, Senegal
Email: gsissoko@yahoo.com

How to cite this paper: Fall, M.F.M., Gaye, I., Diarisso, D., Diop, G., Loum, K., Diop, N., Sy, K.M., Ndiaye, M. and Sissoko, G. (2021) AC Back Surface Recombination Velocity in n^+-p-p^+ Silicon Solar Cell under Monochromatic Light and Temperature. *Journal of Electromagnetic Analysis and Applications*, **13**, 67-81.
https://doi.org/10.4236/jemaa.2021.135005

Received: May 3, 2021
Accepted: May 28, 2021
Published: May 31, 2021

Abstract

Excess minority carrier's diffusion equation in the base of monofaciale silicon solar cell under frequency modulation of monochromatic illumination is resolved. Using conditions at the base limits involving recombination velocities *Sf* and *Sb*, respectively at the junction (n^+/p) and back surface (p^+/p), the AC expression of the excess minority carriers' density $\delta(T, \omega)$ is determined. The AC density of photocurrent J_{ph} (T, ω) is represented versus recombination velocity at the junction for different values of the temperature. The expression of the AC back surface recombination velocity *Sb* of minority carriers is deduced depending on the frequency of modulation, temperature, the electronic parameters $(D(\omega))$ and the thickness of the base. Bode and Nyquist diagrams are used to analyze it.

Keywords

Silicon Solar Cell, AC Back Surface Recombination Velocity, Temperature, Bode and Nyquist Diagrams

1. Introduction

To improve (or control) the quality (performance) of solar cells [1] [2], especially silicon, the recombination parameters of minority carriers, in the bulk (volume) and on interfaces, are the subject of theoretical and experimental investigations [3] [4] [5].

The determination of the recombination in the bulk (lifetime) of minority carriers in the solar cell base [6] [7] is influenced by:

1) The theoretical 1D or 3D study model (crystallography, grain size and thickness of different regions) [8] [9] [10].

2) Recombination at the interfaces, *i.e.*, at the front of the n^+ emitter (*Se*), at junction n^+/p or SCR (*Sf*), on the rear side p/p^+ (*Sb*) of the base [11] [12] [13] [14] [15].

3) The solar cell's operating regime under dark or illumination, can be: steady state [16] [17], transient [18] [19] or frequency dynamics [20] [21].

4) The equivalent electric model associated with the solar cell, according to the operating regime [22] [23].

5) External conditions applied to solar cell *i.e.*: mono or polychromatic illumination [24], temperature (T) [25], electromagnetic field (E, B) [26], irradiation flow (ϕp) by charged particles [27].

It is therefore clear that it is important to carry out the investigations, highlighting, the physical mechanisms of recombination (volume or surface) in each case, and in each region of the solar cell, taking into account the geometric parameters (thickness), in order to dissociate their contribution [28] [29] [30] [31].

Some studies have focused on both the lifetime and the AC back surface recombination velocity of excess minority carriers in the base of the silicon solar cell, in order to dissociate their effects under different external conditions [32] [33].

Our study brings, an exploration by the diagrams of Bode and Nyquist, the AC back surface recombination velocity of minority carriers' expression [34] [35], deduced on a silicon solar cell maintained at temperature (T), illuminated by the front (n^+/p) of the base of thickness (H), by a modulated monochromatic light of short wavelength ($\alpha(\lambda)$).

2. Theoretical Modele

The structure of the n^+-p-p^+ silicon solar cell under front monochromatic illumination [11] [36] in frequency modulation, is given by **Figure 1**.

The excess minority carriers' density $\delta(x,t)$ generated in the base of the solar cell at T temperature and under modulated monochromatic illumination, obeys to the continuity equation [37] [38] [39] given as:

$$D(\omega,T)\times\frac{\partial^2\delta(x,t)}{\partial x^2}-\frac{\delta(x,t)}{\tau}=-G(x,\omega,t)+\frac{\partial\delta(x,t)}{\partial t} \quad (1)$$

The excess minority carriers' density expression in the (p) base, can be written, according to the space coordinates (x) and the time t, as:

$$\delta(x,t)=\delta(x)\cdot e^{-j\omega t} \quad (2)$$

- AC carrier generation rate $G(x,t)$ is given by the relationship:

$$G(x,t)=g(x)\cdot e^{-j\omega t} \quad (3)$$

With the space component [40] written as:

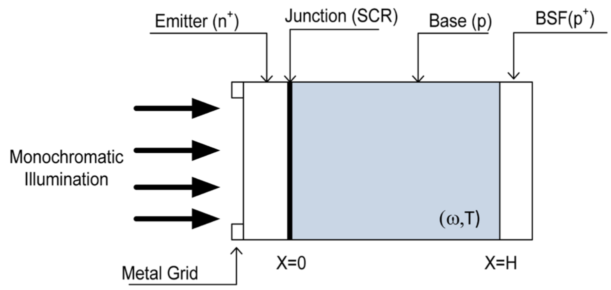

Figure 1. Structure of front illuminated silicon solar cell with monochromatic light.

$$g(x)=\alpha(\lambda)\cdot I_0(\lambda)\cdot(1-R(\lambda))\cdot \mathrm{e}^{-\alpha(\lambda)\cdot x} \tag{4}$$

I_0, is the incident monochromatic flux, $\alpha(\lambda)$ and $R(\lambda)$ are both the absoption and reflection coefficients of the Si material.

- $D(\omega,T)$ is the complex diffusion coefficient of excess minority carrier in the base at T temperature. Its expression is given by the relationship [41]:

$$D(\omega,T)=D(T)\times\left(\frac{1-j\cdot\omega^2\cdot\tau^2}{1+(\omega\tau)^2}\right) \tag{5}$$

$D(T)$ is the temperature-dependent diffusion coefficient given by Einstein's relationship:

$$D(T)=\frac{\mu(T)\cdot K_b\cdot T}{q} \tag{6}$$

T is the temperature in Kelvin, K_b is the Boltzmann constant:

$$K_b=1.38\times10^{-23}\ \mathrm{m}^2\cdot\mathrm{kg}\cdot\mathrm{s}^{-1}\cdot\mathrm{K}^{-1}$$

The mobility coefficient is an important electronic parameter, determinated under many external conditions *i.e.*, temperature [42], magnetic field [43] [44], radiation damage by charged particules [45] [46], doping rate [47]. Thus for electrons, mobility is temperature dependent and expressed by [48] [49]:

$$\mu(T)=1.43\times10^{19}T^{-2.42} \tag{7}$$

By replacing Equations (2) and (3) in Equation (1), the continuity equation for the excess minority carriers' density in the base is reduced to the following relationship:

$$\frac{\partial^2\delta(x,\omega)}{\partial x^2}-\frac{\delta(x,\omega)}{L^2(\omega,T)}=-\frac{g(x)}{D(\omega,T)} \tag{8}$$

$L(\omega,T)$ is the complex diffusion length of excess minority carriers in the base [41] given by:

$$L(\omega,T)=\sqrt{\frac{D(\omega,T)\tau}{1+j\omega\tau}} \tag{9}$$

τ is the excess minority carriers lifetime in the base.

The solution of Equation (8) is:

$$\delta(x,\omega,T) = A\cdot\cosh\left[\frac{x}{L(\omega,T)}\right] + B\cdot\sinh\left[\frac{x}{L(\omega,T)}\right] + K\cdot e^{-\alpha\cdot x} \tag{10}$$

$$\text{With}\quad K = \frac{\alpha\cdot I_0\cdot(1-R)\cdot\left[L(\omega,T)\right]^2}{D(\omega,T)\left[L(\omega,T)^2\cdot\alpha^2-1\right]}\quad\text{and}\quad L(\omega,T)^2\cdot\alpha^2\neq 1 \tag{11}$$

Coefficients A and B are determined through the boundary conditions:

- At the junction (n⁺/p) ($x = 0$)

$$D(\omega,T)\frac{\partial\delta(x,T)}{\partial x}\bigg|_{x=0} = Sf\cdot\frac{\delta(x,T)}{D(\omega,T)}\bigg|_{x=0} \tag{12}$$

- On the back side (p/p+) in the base ($x = H$)

$$D(\omega,T)\frac{\partial\delta(x,T)}{\partial x}\bigg|_{x=H} = -Sb\cdot\frac{\delta(x,T)}{D(\omega,T)}\bigg|_{x=H} \tag{13}$$

Sf and *Sb* are excess minority carrier recombination velocity respectively at the junction and at the back surface.

The variation of recombination velocity *Sf*, through Equation (12) describes the solar cell operating point that is imposed by the external load [12] [14]. Intrinsic *Sf* component describing the carrier losses, is then associated with the shunt resistor though the solar cell electrical equivalent model [50] [51] [52].

The excess minority carrier recombination velocity *Sb* on the back surface is associated with the p/p⁺ junction which generates an electric field, for throwing back the charge carrier toward the junction [14] [15] [36] and then increases their collection.

3. Results and Discussions

3.1. Photocurrent

The density of photocurrent at the junction is obtained from the density of minority carriers in the base and is given by the following expression:

$$J_{ph}(Sf,Sb,\omega,T) = qD(\omega,T)\frac{\partial\delta(x,Sf,Sb,\omega,T)}{\partial x}\bigg|_{x=0} \tag{14}$$

where q is the elementary electron charge.

Figure 2 shows AC photocurrent versus the junction surface recombination velocity for different temperature.

3.2. AC Back Surface Recombination Velocity *Sb*

For a given frequency, the representation of AC photocurrent density versus junction minority carrier's recombination velocity shows the short-circuit current density (J_{phsc}) for very large *Sf* values, where obviously we can write [13] [14] [35]:

$$\frac{\partial J_{ph}(Sf,Sb,\omega,T,\alpha(\lambda))}{\partial Sf}\bigg|_{Sf\geq 10^5\,\text{cm}\cdot\text{s}^{-1}} = 0 \tag{15}$$

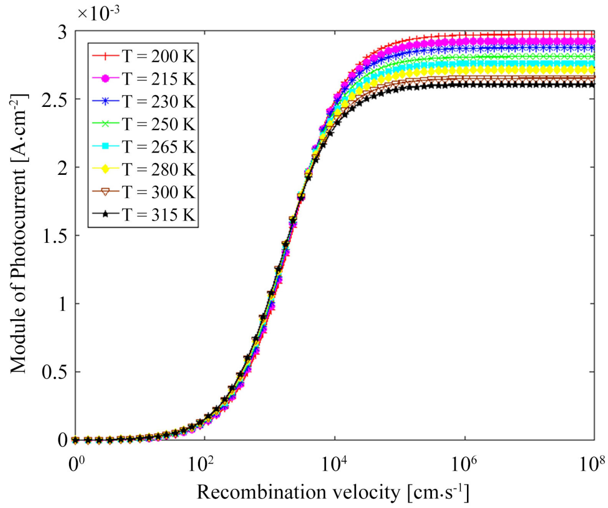

Figure 2. Photocurrent density versus junction surface recombination velocity under temperature influence. ($\omega = 10^5$ rad/s; $H = 0.025$ cm; $\alpha = 6.2$ cm^{-1}).

The solution of this Equation (15) leads to expressions of the AC recombination velocity in the back surface, given by [53]:

$$Sb1(\omega,T,\alpha(\lambda)) = \frac{D(\omega,T)}{L(\omega,T)} \cdot \left[\frac{\alpha(\lambda)\cdot L(\omega,T)\cdot\left(\exp(-\alpha(\lambda)\cdot H) - \cosh\left(\frac{H}{L(\omega,T)}\right) + \sinh\left(\frac{H}{L(\omega,T)}\right)\right)}{\exp(-\alpha(\lambda)\cdot H) - \cosh\left(\frac{H}{L(\omega,T)}\right) + \alpha(\lambda)\cdot L(\omega,T)\cdot \sinh\left(\frac{H}{L(\omega,T)}\right)} \right] \quad (16)$$

$$Sb2(\omega,T) = -\frac{D(\omega,T)}{L(\omega,T)} \cdot \tanh\left(\frac{H}{L(\omega,T)}\right) \quad (17)$$

3.3. Amplitude and Phase (Bode Diagrams)

Previous studies have focused on the second solution given to the Equation (17) [32] [33] [34]. Our study will consider the second solution (Equation (16) [54] whose module and phase are represented versus logarithm of the modulation frequency by **Figure 3** and **Figure 4** for different temperature and long wavelength (λ) corresponding to low absorption coefficient value (α = 6.02 cm^{-1}), characterized by deep penetration in the base ($\alpha L(\omega) \ll 1$) [16] [24] [53] [55].

Sbampl (ω, T) and $\phi(\omega, T)$ correspond, for a given temperature T, to the amplitude and phase component of *Sb*. At low frequencies (≤10^4 rad/s), the stationary regime is observed and gives constant amplitudes that decrease with temperature T (**Figure 3**).

The (Ac) *Sb* recombination velocity at the rear face in complex form (real and imaginary components, with a complex number (J)) is presented by analogy with the Maxwell-Wagner-Sillars model (MWS) [56] and can be written as:

$$Sb(\omega,T) = Sb'(\omega,T) + J \cdot Sb''(\omega,T) \quad (18)$$

The alternative phase (**Figure 4**) for a given temperature, is written:

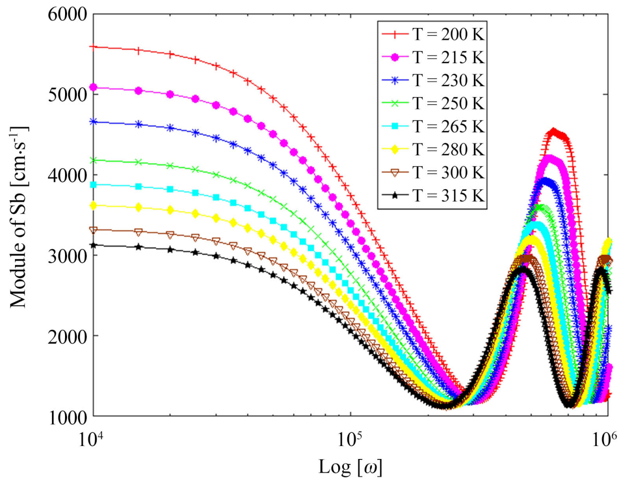

Figure 3. Module of *Sb* versus frequency for different temperature ($H = 0.025$ cm; $\alpha = 6.2$ cm^{-1}).

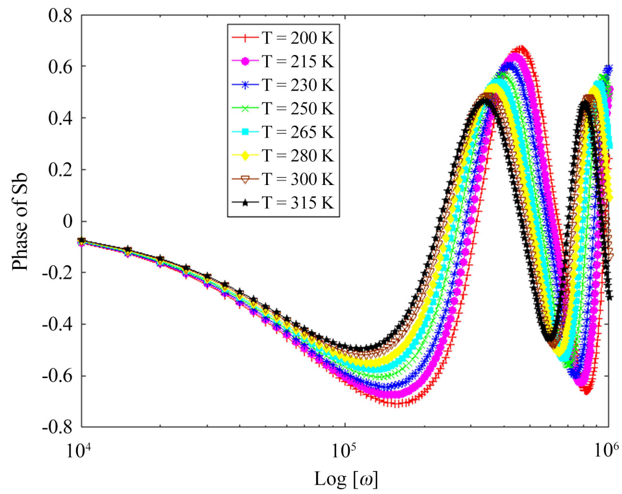

Figure 4. Phase of Sb versus frequency for different temperature ($H = 0.025$cm; $\alpha = 6.2$ cm^{-1}).

$$\tan\left(\phi(\omega,T)\right) = \frac{Sb''(\omega,T)}{Sb'(\omega,T)} \tag{19}$$

The phase of the recombination velocity is negative at low values of the pulse. At large frequencies (ω less than 10^5 rad/s), it is presented as a damped sine wave, with amplitude and resonant frequency decreasing with temperature.

The positive and negative semicircles correspond respectively to small and large diameters of the Nyquist diagram and allow to conclude on the equivalent electrical model characterizing the AC *Sb* recombination velocity [33] [34] [35] [57].

3.4. Niquyst Diagram of the Recombination Velocity

The Nyquist diagram which is the representation of the imaginary part of *Sb* as a function of the real part, for different temperatures.

Figure 5 and with a zoom represented by **Figure 6** show semicircles, of different diameters, which decrease with temperature. The semicircles corresponding to *Sb*" positive imaginary (*ReSb*(*ind*)) are of smaller diameters than those corresponding to *Sb*" negative imaginary (*ImSb*(*cap*)).

The quantities (*ReSb*(*cap*)) and (*ImSb*(*ind*)) represent the inductive and capacitive effects (dominant effect) of the recombination velocity of the minority charge carriers, for each temperature.

An intersection point (*Sb*') of each semicircle with the real (horizontal) axis of *Sb* is observed. This offset (shift) from the origin of the axes narrows with temperature. This difference is the real part of the recombination velocity of the minority charge carriers, for each temperature represents the resistive part [33] [34] [35] [51] [57] [58].

The quantities (*ImSb*(*cap*)), (*ImSb*(*ind*)) and (*Sb*') are extracted, for each temperature and presented in the **Table 1**.

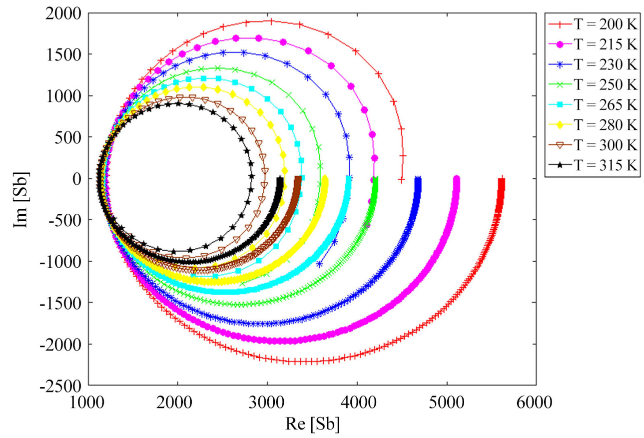

Figure 5. Imaginary component versus real component of *Sb* for different temperature ($H = 0.025$ cm; $\alpha = 6.2$ cm^{-1}).

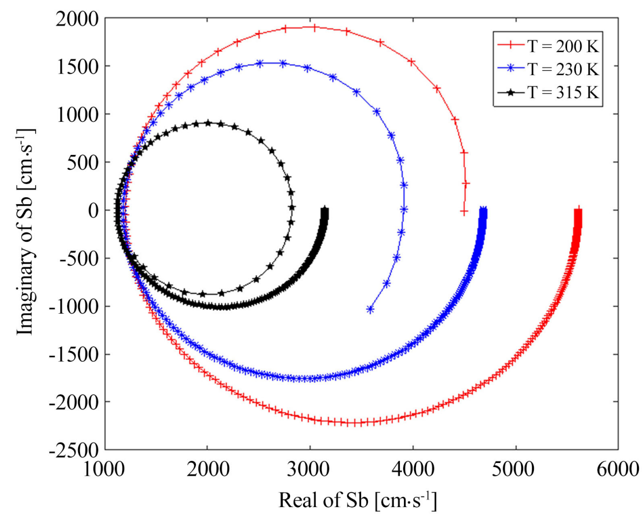

Figure 6. Imaginary component versus real component of *Sb* for different temperature ($H = 0.025$ cm; $\alpha = 6.2$ cm^{-1}).

Table 1. Shif part, maximum amplitude of both the imaginary and real parts of *Sb* for different temperature values.

T (K)	200	215	230	250	265	280	300	315
$Re(Sb)$	203	193	182	170	159	148	134	124
$Re(Sb)cap$	4415	3917	3499	3035	2744	2492	2205	2018
$Im(Sb)cap$	2214	1965	1755	1523	1377	1251	1106	1013
$Re(Sb)ind$	3294	2991	2729	2417	2223	2046	1837	1700
$Im(Sb)ind$	1900	1694	1521	1332	1210	1101	977.3	901.2

Figures 7-11, are drawn from the Table 1. Figure 7 shows the representation of ($Re(Sb)$), the real part (Sb') as a function of temperature, which reflects the resistive (ohmic) effect associated with the recombination velocity Sb of minority carriers.

$$Re(Sb) = -0.69 \times T(\mathrm{K}) + 3.4 \times 10^2 \tag{20}$$

The modeling expression in Figure 7 shows the decreasing line of $Re(Sb)$ with temperature. This quantity is associated with the resistive behavior of the recombination velocity on the rear face [50] [51] [59]. The increase in temperature reduces the loss of minority carriers and reinforces the BSF character of the junction (p/p^+) on the rear face.

Figure 8 and Figure 10 give the reciprocal of both, the real parts $Sb(cap)$ and $Sb(ind)$, respectively of Sb", as a function of temperature. While Figure 9 and Figure 11, produce the reciprocal representations of the imaginary parts of $Sb(cap)$ and $Sb(ind)$, as a function of temperature.

$$1/Re(Sb)cap = 2.3 \times 10^{-6} \times T(\mathrm{K}) - 0.00025 \tag{21}$$

$$1/Im(Sb)cap = 4.7 \times 10^{-6} \times T(\mathrm{K}) - 0.00049 \tag{22}$$

$$1/Re(Sb)ind = 2.5 \times 10^{-6} \times T(\mathrm{K}) - 0.0002 \tag{23}$$

$$1/Im(Sb)cap = 5.1 \times 10^{-6} \times T(\mathrm{K}) - 0.0005 \tag{24}$$

Figures 8-11 show increasing lines with the rise in temperature associated with the Umklapp process which acts on the diffusion coefficient of minority carriers [33] [60] [61] [62]. Modeling expressions are given through Equations (21)-(24).

Figure 8 and Figure 10 show that the capacitive and inductive effects resulting from the imaginary part of Sb are not perfect and therefore reflect the ohmic losses (or leaks).

On the other hand, Figure 9 and Figure 11 are associated respectively with a purely capacitive and inductive behavior of the minority carrier recombination velocity, by storage or discharge towards the junction (n^+/p).

The AC recombination velocity (Sb), can be presented, through its equivalent electric model like a pure resistance (associated with $Re(Sb)$), in series with both imperfect capacitor (capacitor in parrallel with resistor) and inductance (inductance in parallel with a resistor) undergoing the effects of the temperature [25] [34] [63].

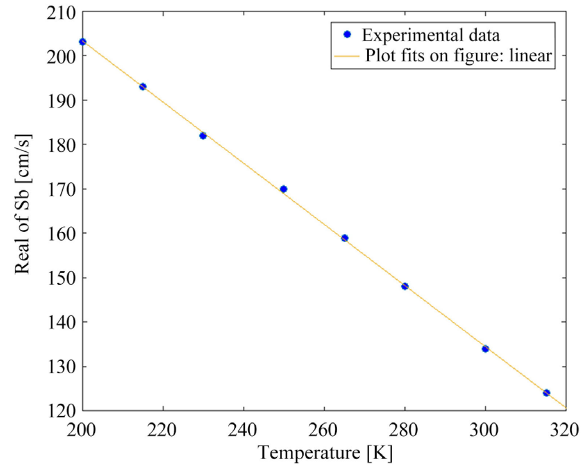

Figure 7. Real of *Sb* versus temperature.

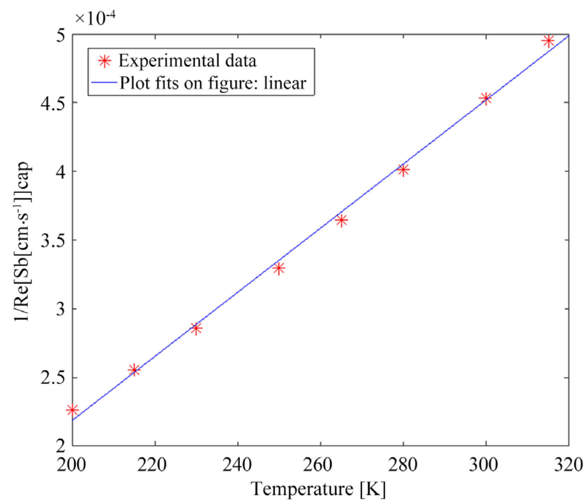

Figure 8. Reciprocal of *Sb* real (capacitance) versus temperature.

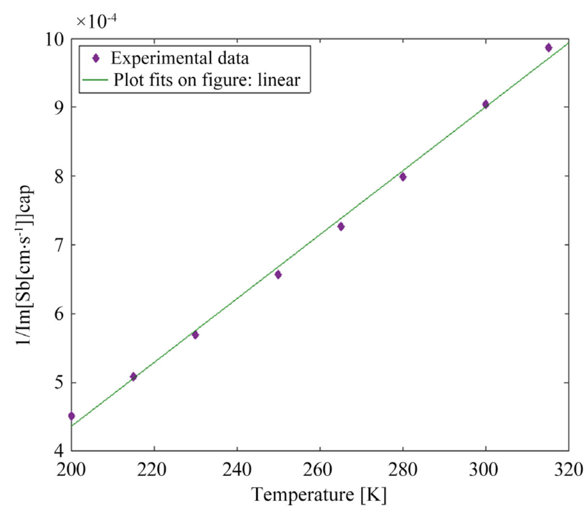

Figure 9. Reciprocal of *Sb* imaginary (capacitance) versus temperature.

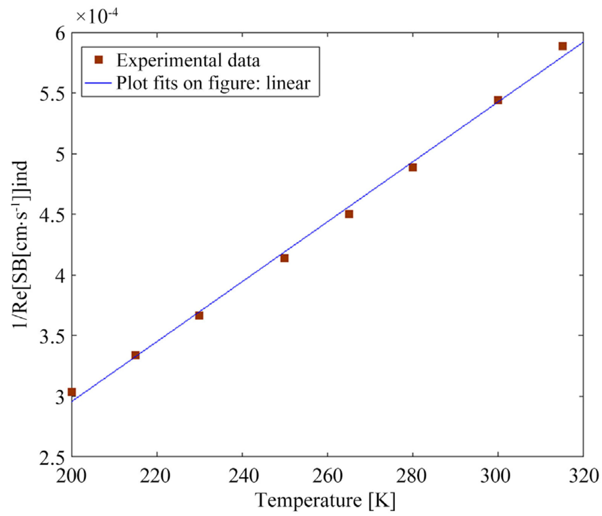

Figure 10. Reciprocal of *Sb* real (inductance) versus temperature.

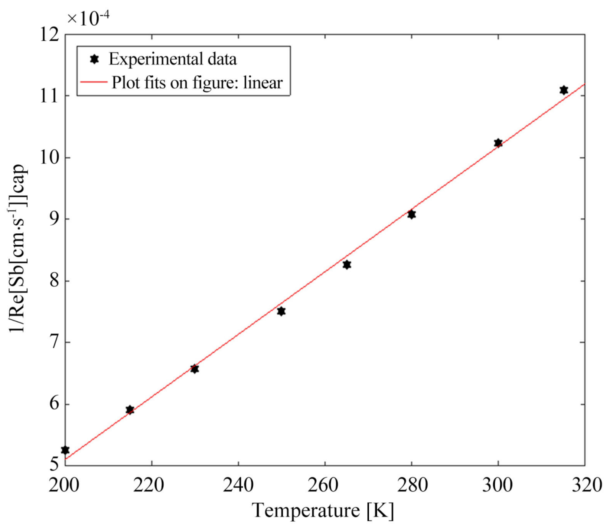

Figure 11. Reciprocal of *Sb* imaginary (inductance) versus temperature.

4. Conclusions

This study of the mono-facial silicon solar cell ($n^+/p/p^+$) under temperature and under monochromatic illumination in frequency modulation, made it possible to extract the theoretical expression AC of the recombination velocity of minority carriers on the rear face (p/p^+), at long wavelengths giving deep penetration (low absorption coefficient) of the wave.

The analysis of this AC recombination velocity, at different temperatures, through the diagrams of Boode (amplitude and phase) and Nyquist, led to an equivalent electrical model, suggesting, a series resistance associated with both imperfect capacitor and an inductive winding in series. At low frequencies (static regime), whatever the temperature, the resistive effect of the AC Sb is preponderant.

Conflicts of Interest

The authors declare no conflicts of interest regarding the publication of this paper.

References

[1] Martin, A.G. (1995) Silicon Solar Cells Advanced Principles & Practice. Center for Photovoltaic Devices & Systems.

[2] Yadav, P., Pandey, K., Tripathi, B., Kumar, C.M., Srivastava, S.K., Singh, P.K. and Kumar, M. (2015) An Effective Way to Analyze the Performance Limiting Parameters of a Poly-Crystalline Silicon Solar Cell Fabricated in the Production Line. *Solar Energy*, **122**, 1-10. https://doi.org/10.1016/j.solener.2015.08.005

[3] Liou, J.J. and Wong, W.W. (1992) Comparison and Optimization of the Performance of Si and GaAs Solar Cells. S*olar Energy Materials and Solar Cells*, 28, 9-28. https://doi.org/10.1016/0927-0248(92)90104-W

[4] Takahashi, Y., Kondo, H., Yamazaki, T., Uraoka, Y. and Fuyuki, T. (2007) Precise Analysis of Surface Recombination Velocity in Crystalline Silicon Solar Cells Using Electroluminescence. *Japanese Journal of Applied Physics*, **46**, 1149-1151. https://doi.org/10.1143/JJAP.46.L1149

[5] De Vischere, P. (1986) Comment on G. J. Rees. "Surface Recombination Velocity—A Useful Concept?" *Solid State Electronics*, **29**, 1161-1164. https://doi.org/10.1016/0038-1101(86)90059-6

[6] Dhariwal, S.R. and Vasu, N.K. (1981) A Generalized Approach to Lifetime Measurement in *pn* Junction Solar Cells. *Solid-State Electronics*, **24**, 915-927. https://doi.org/10.1016/0038-1101(81)90112-X

[7] Jain, S.C. (1983) The Effective Lifetime in Semicrystalline Silicon. *Solar Cells*, **9**, 345-352. https://doi.org/10.1016/0379-6787(83)90028-5

[8] Barro, F.I., Mbodji, S., Ndiaye, M., Ba, E. and Sissoko, G. (2008) Influence of Grains Size and Grains Boundaries Recombination on the Space-Charge Layer Thickness z of Emitter-Base Junction's n^+-p-p^+ Solar Cell. *Proceedings of* 23*rd European Photovoltaic Solar Energy Conference and Exhibition*, Valencia 1-5 September, 604-607.

[9] Diallo, H.L., Ly, I., Zoungrana, M., Nzonzolo, Barro, F.I. and Sissoko, G. (2006) 3D Modeling of a Bifacial Polycrystalline Silicon Solar Cell in Order to Exhibite the Effect of Grain Size and Grain Boundary on the Recombination Parameters under a Constant White Illumination. *Proceedings of the* 21*st European Photovoltaic Solar Energy Conference and Exhibition*, Dresden, 4-8 September 2006, 451-454.

[10] Caleb Dhanasekaran, P. and Gopalam, B.S.V. (1981) Effect of Junction Depth on the Performance of a Diffused n^+p Silicon Solar Cell. *Solid State Electrons*, **24**, 1077-1080. https://doi.org/10.1016/0038-1101(81)90172-6

[11] Rose, B.H. and Weaver, H.T. (1983) Determination of Effective Surface Recombination Velocity and Minority Carrier Lifetime in High-Efficiency Si Solar Cells. *Journal of Applied Physics*, **54**, 238-247. https://doi.org/10.1063/1.331693

[12] Sissoko, G., Sivoththanam, S., Rodot, M. and Mialhe, P. (1992) Constant Illumination-Induced Open Circuit Voltage Decay (CIOCVD) Method, as Applied to High Efficiency Si Solar Cells for Bulk and Back Surface Characterization. 11*th European Photovoltaic Solar Energy Conference and Exhibition*, Montreux, 12-16 October 1992, 352-354.

[13] Sissoko, G., Museruka, C., Corréa, A., Gaye, I. and Ndiaye, A.L. (1996) Light Spectral Effect on Recombination Parameters of Silicon Solar Cell. *World Renewable*

Energy Congress, Pergamon, 15-21 June 1996, 1487-1490.

[14] Diallo. H.L, Maiga, S.A., Wereme, A. and Sissoko, G. (2008) New Approach of Both Junction and Back Surface Recombination Velocities in a 3D Modelling Study of a Polycrystalline Silicon Solar Cell. *The European Physical Journal Applied Physics*, **42**, 203-211. https://doi.org/10.1051/epjap:2008085

[15] Fossum, J.G. (1977) Physical Operation of Back-Surface-Field Silicon Solar Cells. *IEEE Transactions on Electron Devices*, **2**, 322-325. https://doi.org/10.1109/T-ED.1977.18735

[16] Stokes, E.D. and Chu, T.L. (1977) Diffusion Lengths in Solar Cells from Short-Circuit Current Measurements. *Applied Physics Letters*, **30**, 425-426. https://doi.org/10.1063/1.89433

[17] Jain, G.C., Singh, S.N. and Kotnala, R.K. (1983) Diffusion Length Determination in n^+-p-p^+ Structure Based Silicon Solar Cells from the Intensity Dependence of the Short-Circuit Current For Illumination from the p^+ Side. *Solar Cells*, **8**, 239-248. https://doi.org/10.1016/0379-6787(83)90063-7

[18] Jung, T.-W., Lindholm, F.A. and Neugroschel, A. (1984) Unifying View of Transient Responses for Determining Lifetime and Surface Recombination Velocity in Silicon Diodes and Back-Surface-Field Solar Cells, with Application to Experimental Short-Circuit-Current Decay. *IEEE Transactions on Electron Devices*, **31**, 588-595. https://doi.org/10.1109/T-ED.1984.21573

[19] Kunst, M., Muller, G., Schmidt, R. and Wetzel, H. (1988) Surface and Volume Decay Processes in Semiconductors Studied by Contactless Transient Photoconductivity Measurements. *Applied Physics A*, **46**, 77-85. https://doi.org/10.1007/BF00615912

[20] Mora-Sero, I., Garcia-Belmonte, G., Boix, P.P., Vazquez, M.A. and Bisquert, J. (2009) Impedance Spectroscopy Characterization of Highly Efficient Silicon Solar Cells under Different Illumination Intensities Light. *Energy and Environmental Science*, **2**, 678-686. https://doi.org/10.1039/b812468j

[21] Sahin, G., Dieng, M., Moujtaba, M., Ngom, M., Thiam, A. and Sissoko, G. (2015) Capacitance of Vertical Parallel Junction Silicon Solar Cell under Monochromatic Modulated Illumination. *Journal of Applied Mathematics and Physics*, **3**, 1536-1543. https://doi.org/10.4236/jamp.2015.311178

[22] Lovejoy, M.L., Melloch, M.R., Ahrenkiel, R.K. and Lundstrom, M.S. (1992) Measurement Considerations for Zero-Field Time-of-Flight Studies of Minority Carrier Diffusion in III-V Semiconductors. *Solid-State Electronics*, **35**, 251-259. https://doi.org/10.1016/0038-1101(92)90229-6

[23] El-Basit, W.A., Abd El-Maksood, A.M. and El-Moniem Saad Soliman, F.A. (2013) Mathematical Model for Photovoltaic Cells. *Leonardo Journal of Sciences*, **23**, 13-28. http://ljs.academicdirect.org

[24] Antilla, O.J. and Hahn, S.K. (1993) Study on Surface Photovoltage Measurement of Long Diffusion Length Silicon: Simulation Results. *Journal of Applied Physics*, **74**, 558-569https://doi.org/10.1063/1.355343

[25] Denise, K., Mamadou, L.B., Mamour, A.B., Gora, D., El Hadj, S., Oulimata, M. and Gregoire, S. (2020) AC Back Surface Recombination in n+-p-p+ Silicon Solar Cell: Effect of Temperature. *International Journal of advanced Research* (*IJAR*), **8**, 140-151. https://doi.org/10.21474/IJAR01/11273

[26] Diao, A., Wade, M., Thiame, M. and Sissoko, G. (2017) Bifacial Silicon Solar Cell Steady Photoconductivity under Constant Magnetic Field and Junction Recombination Velocity Effects. *Journal of Modern Physics*, **8**, 2200-2208.

https://doi.org/10.4236/jmp.2017.814135

[27] Ba, M.L., Thiam, N., Thiame, M., Traore, Y., Diop, M.S., Ba, M., Sarr, C.T., Wade, M. and Sissoko, G. (2019) Base Thickness Optimization of a (n^+-p-p^+) Silicon Solar Cell in Static Mode under Irradiation of Charged Particles. *Journal of Electromagnetic Analysis and Applications*, **11**, 173-185. https://doi.org/10.4236/jemaa.2019.1110012

[28] Demesmaeker, E., Symons, J., Nijs, J. and Mertens, R. (1991) The Influence of Surface Recombination on the Limiting Efficiency and Optimum Thickness of Silicon Solar Cells. 10*th European Photovoltaic Solar Energy Conference*, Lisbon, 8-12 April 1991, 66-67. https://doi.org/10.1007/978-94-011-3622-8_17

[29] Gaubas, E. and Vanhellemont, J. (1996) A Simple Technique for the Separation of Bulk and Surface Recombination Parameters in Silicon. *Journal of Applied Physics*, **80**, 6293-6297. https://doi.org/10.1063/1.363705

[30] Noriaki, H. and Chusuke, M. (1987) Sample Thickness Dependence of Minority Carrier Lifetimes Measured Using an AC Photovoltaic Method. *Japanese Journal of Applied Physics*, Vol. 26, **12**, 2033-2036. https://doi.org/10.1143/JJAP.26.2033

[31] Van Steenwinkel, R., Carotta, M.C., Martinelli, G., Mercli, M., Passari, L. and Palmeri, D. (1990) Lifetime Measurement in Solar Cell of Various Thickness and Related Silicon Wafer. *Solar Cells*, **28**, 287-292. https://doi.org/10.1016/0379-6787(90)90063-B

[32] Ndiaye, A., Gueye, S., Sow, O., Diop, G., Ba, A., Ba, M., Diatta, I., Habiboullah, L. and Sissoko, G. (2020) A.C. Recombination Velocity as Applied to Determine n^+/p/p^+ Silicon Solar Cell Base Optimum Thickness. *Energy and Power Engineering*, **12**, 543-554. https://doi.org/10.4236/epe.2020.1210033

[33] Traore, Y., Thiam, N., Thiame, M., Ba, M.L., Diouf, M.S. and Sissoko, G. (2019) AC Recombination Velocity in the Back Surface of a Lamella Silicon Solar Cell under Temperature. *Journal of Modern Physics,* **10**, 1235-1246. https://doi.org/10.4236/jmp.2019.1010082

[34] Ly Diallo, H., Wade, M., Ly, I., NDiaye, M., Dieng, B., Lemrabott, O.H., Maïga, A.S. and Sissoko. G. (2012) 1D Modeling of a Bifacial Silicon Solar Cell under Frequency Modulation, Monochromatic Illumination: Determination of the Equivalent Electrical Circuit Related to the Surface Recombination Velocity. *Research Journal of Applied Sciences*, *Engineering and Technology*, **4**, 1672-1676. http://www.maxwell.org

[35] Ly, I., Zerbo, I., Wade, M., Ndiaye, M., Dieng, A., Diao, A., Thiam, N., Thiam, A., Dione, M.M., Barro, F.I., Maiga, A.S. and Sissoko, G. (2011) Bifacial Silicon Solar Cell under Frequency Modulation and Monochromatic Illumination: Recombination Velocities and Associated Equivalent Electrical Circuits. *Proceedings of* 26*th European Photovoltaic Solar Energy Conference and Exhibition*, Hamburg, 5-9 September 2011, 298-301.

[36] Nam, L.Q., *et al.* (1992) Solar Cells with 15.6% Efficiency on Multicrystalline Silicon, Using Impurity Gettering Back Surface Field and Emitter Passivation. *International Journal of Solar Energy*, **11**, 273-279. https://doi.org/10.1080/01425919208909745

[37] Mandelis, A., Ward, A. and Lee, K.T. (1989) Combined AC Photocurrent and Photothermal Reflectance Response Theory of Semiconducting p-n Junctions. *Journal of Applied Physics*, **66**, 5572-5583. https://doi.org/10.1063/1.343662

[38] Sudha, G., Feroz, A. and Suresh, G. (1988) A Method for the Determination of the Material Parameters, D, L_o, S and α from Measured A.C. Short-Circuit Photocurrent. *Solar Cells*, **25**, 61-72. https://doi.org/10.1016/0379-6787(88)90058-0

[39] Wang, C.H. and Neugroschel, A. (1991) Minority-Carrier Lifetime and Surface Recombination Velocity Measurement by Frequency-Domain Photoluminescence. *IEEE*

Transactions on Electron Devices, **38**, 2169-2180. https://doi.org/10.1109/16.83745

[40] Meier, D.L., Hwang, J.-M. and Campbell, R.B. (1988) The Effect of Doping Density and Injection Level on Minority Carrier Lifetime as Applied to Bifacial Dendritic Web Silicon Solar Cells. *IEEE Transactions on Electron Devices*, **35**, 70-79. https://doi.org/10.1109/16.2417

[41] Luc, B., Shahriar, M., Dean, H., Marco, S., Manuela, A. and Claudio, N. (1994) Investigation of Carrier Transport through Silicon Wafers by Photocurrent Measurement. *Journal of Applied Physics*, **75**, 4000-4008. https://doi.org/10.1063/1.356022

[42] Misiakos, K. and Tsamakis, D. (1994) Electron and Hole Mobilities in Lightly Doped Silicon. *Applied Physics Letters*, **64**, 2007-2009. https://doi.org/10.1063/1.111721

[43] Bester, Y., Bester, Y., Ritter, D., Bahia, G., Cohen, S. and Sparkling, J. (1995) Method Measurement of the Minority Carrier Mobility in the Base of Heterojunction Bipolar Transistor Using a Magneto transport Method. *Applied Physics Letters*, **67**, 1883-1884. https://doi.org/10.1063/1.114364

[44] Vardanyan, R.R., Kerst, U., Wawer, P., Nell, M.E. and Wagemann, H.G. (1998) Method for Measurement of All Recombination Parameters in the Base Region of Solar Cells. 2*nd World Conference and Exhibition on Photovoltaic Solar Energy Conversion*, Vienna, 6-10 July 1998, 191-193.

[45] Rosenzweig, W. (1962) Diffusion Length Measurement by Mean of Ionization Radiation. *The Bell System Technical Journal*, **41**, 1573-1588. https://doi.org/10.1002/j.1538-7305.1962.tb03995.x

[46] Arora, N.D. and Hauser, J.R. (1982) Temperature Dependence of Silicon Solar Cell Characteristics. *Solar Energy Materials*, **6**, 151-158. https://doi.org/10.1016/0165-1633(82)90016-8

[47] Dione, M.M., Diao, A., Ndiaye, M., Ly Diallo, H., Thiam, N., Barro, F.I., Wade, M., Maiga, A.S. and Sissoko, G. (2010) 3D Study of a Monofacial Silicon Solar Cell under Constant Monocrhomatic Light: Influence of Grain Size, Grain Boundary Recombination Velocity, Illumination Wavelength, Back Surface and Junction Recombination Velocities. *Proceedings of* 25*th European Photovoltaic Solar Energy Conference and Exhibition*, Valencia, 6-9 September 2010, 488-491.

[48] Dorkel, J.M. and Leturcq, P. (1981) Carrier Mobilities in Silicon Solar Semi-Empirically Related Temperature, Doping and Injection Level. *Solid State Electron*, **24**, 821-825. https://doi.org/10.1016/0038-1101(81)90097-6

[49] Thurmond, C.D. (1975) The Standard Thermodynamic Functions for the Formation of Electron and Hole in Ge, Si, GaAs and GaP. *Journal of The Electrochemical Society*, **122**, 133-41. https://doi.org/10.1149/1.2134410

[50] El Hadji, N., Sahin, G., Thiam, A., Dieng, M., Ly Diallo, H., Ndiaye, M. and Sissoko, G. (2015) Study of the Intrinsic Recombination Velocity at the Junction of Silicon Solar under Frequency Modulation and Irradiation. *Journal of Applied Mathematics and Physics*, **3**, 1522-1535. https://doi.org/10.4236/jamp.2015.311177

[51] Fatimata, B., Boureima, S., Mamadou, W., Marcel, S.D., Brahima, L. and Grégoire, S. (2016) Equivalent Electric Model of the Junction Recombination Velocity limiting the Open Circuit of a Vertical Parallel Junction Solar Cell under Frequency Modulation. *IPASJ International Journal of Electronics & Communication* (*IIJEC*), **4**, 1-11.

[52] Diasse, O., Diao, A., Ly, I., Diouf, M.S., Diatta, I., Mane, R., Traore, Y. and Sissoko, G. (2018) Back Surface Recombination Velocity Modeling in White Biased Silicon Solar Cell under Steady State. *Journal of Modern Physics*, **9**, 189-201. https://doi.org/10.4236/jmp.2018.92012

[53] Zerbo, I., Barro, F.I., Mbow, B., Diao, A., Madougou, S., Zougmore, F. and Sissoko, G. (2004) Theoretical Study of Bifacial Silicon Solar Cell under Frequency Modulate white Light: Determination of Recombination Parameters. *Proceedings of the* 19*th European Photovoltaic Solar Energy Conference*, Paris, 7-11 June 2004, 258-261.

[54] Thiam, N., Diao, A., Ndiaye, M., Dieng, A., Thiam, A., Sarr, M., Maiga, A.S. and Sissoko, G. (2012) Electric Equivalent Models of Intrinsic Recombination Velocities of a Bifacial Silicon Solar Cell under Frequency Modulation and Magnetic Field Effect. *Research Journal of Applied Sciences*, *Engineering and Technology*, **4**, 4646-4655. https://doi.org/10.19026/rjaset.5.4825

[55] Rajman, K., Singh, R. and Shewchun, J. (1979) Absorption Coefficient for Solar Cell Calculations. *Solid State Electronics*, **22**, 793-795. https://doi.org/10.1016/0038-1101(79)90128-X

[56] Maxwell, J.C. (1982) Electricity and Magnetism. Calerdon, Oxford.

[57] Diao, A., Thiam, N., Zoungrana, M., Sahin, G., Ndiaye, M. and Sissoko, G. (2014) Diffusion Coefficient in Silicon Solar Cell with Applied Magnetic Field and under Frequency: Electric Equivalent Circuits. *World Journal of Condensed Matter Physics*, **4**, 84-92. https://doi.org/10.4236/wjcmp.2014.42013

[58] Anil Kumar, R., Suresh, M.S. and Nagaraju, J. (2001) Measurement of AC Parameters of Gallium Arsenide (GaAs/Ge) Solar Cell by Impedance Spectroscopy. *IEEE Transaction on Electron Devices*, **48**, 2177-2179. https://doi.org/10.1109/16.944213

[59] Mohamadou, S.N., Boureima, S., Ibrahima, L., Marcel, S.D., Mamadou, W., Senghane, M. and Grégoire, S. (2016) Irradiation Effect on Silicon Solar Cell Capacitance in Frequency Modulation. *International Journal of Innovative Technology and Exploring Engineering* (*IJITEE*), **6**, 2278-3075.

[60] Richard, M., Ibrahima, L., Mamadou, W., Ibrahima, D., Marcel, S.D., Youssou, T., Mor, N., Seni, T. and Grégoire, S. (2017) Minority Carrier Diffusion Coefficient D*(B, T): Study in Temperature on a Silicon Solar Cell under Magnetic Field. *Energy and Power Engineering*, **9**, 1-10. http://www.scirp.org/journal/epe https://doi.org/10.4236/epe.2017.91001

[61] Seydina, D., Mor, N., Ndeye, T., Youssou, T., Mamadou, L.B., Ibrahima, D., Marcel, S.D., Oulimata, M., Amary, T. and Grégoire, S. (2019) Influence of Temperature and Frequency on Minority Carrier Diffusion Coefficient in a Silicon Solar Cell Under Magnetic Field. *Energy and Power Engineering*, **11**, 355-361. https://doi.org/10.4236/epe.2019.1110023

[62] Gueye, M., Diallo, H.L., Kosso, A., Moustapha, M., Traore, Y., Diatta I. and Sissoko, G. (2018) AC Recombination Velocity in a Lamella Silicon Solar Cell. *World Journal of Condensed Matter Physics*, **8**, 185-196,http://www.scirp.org/journal/wjcmp. https://doi.org/10.4236/wjcmp.2018.84013

[63] Fabrick, L.B. and Eskenas, K.L. (1985) Admittance Spectroscopy and Application to $CuInSe_2$ Photovoltaic Devices. *In Proc of the IEEE PVSC*, Las Vegas, 21-25 October 1685, 754-757.